Left Ventricular Systolic and Diastolic Dysfunction after Infusion of Tumor Necrosis Factor-α in Conscious Dogs

Francis D. Pagani, Lauren S. Baker, Charles Hsi, Mark Knox, Mitchell P. Fink, and Marc S. Visner†
University of Massachusetts Medical Center, Department of Surgery, Worcester, Massachusetts 01655

Abstract

We used a load-insensitive index of systolic left ventricular (LV) function and an analysis of diastolic pressure–dimension relationships to test the hypothesis that recombinant human (rh) tumor necrosis factor-α (TNFα) impairs LV function in dogs. Animals were studied 7–10 d after aseptic implantation of instrumentation to monitor cardiac output, external anterior-posterior LV diameter, and LV and pleural pressures. Data were analyzed from seven dogs that received active rhTNFα (100 μg/kg over 60 min) and from five dogs that received heat-inactivated rhTNFα. At 24 h after infusion of active rhTNFα, the slope of the LV end-diastolic dimension–stroke work relationship decreased significantly, indicating a decrement in LV systolic contractility. Simultaneously, LV unstressed dimension increased significantly, suggesting diastolic myocardial creep. The end-diastolic relationship between LV transmural pressure and normalized LV dimension (strain) was markedly displaced to the left, suggesting increased diastolic elastic stiffness. Despite these changes in LV performance, cardiac index was maintained by tachycardia. The abnormalities in LV function were resolved by 72 h. We conclude that rhTNFα reversibly impairs LV systolic and diastolic function in unanesthetized dogs. Because dysfunction occurs > 6 h after the infusion of rhTNFα and persists for 24–48 h, the mechanism underlying this phenomenon may involve secondary mediators or a change in myocardial gene expression. (*J. Clin. Invest.* 1992. 90:389–398.) Key words: cytokine • myocardial contractility • myocardial blood flow • myocardial creep • myocardial stiffness

Introduction

Recent clinical and experimental studies strongly support the hypothesis that tumor necrosis factor-α (TNFα)[1] is a mediator of organ dysfunction and shock induced by sepsis and endotox-

emia. Elevated plasma levels of TNFα are present in patients with a variety of infectious diseases (1), and plasma levels of TNFα correlate with morbidity and mortality due to meningicoccal meningitis (2). Administration of lipopolysaccharide (LPS) to humans (3) or animals (4, 5), and infusion of live bacteria in animals (6, 7) increases plasma levels of TNFα. Administration of TNFα to humans (8, 9), mice (10, 11), rats (12–16), rabbits (17), dogs (18–20), and sheep (21, 22) elicits manifestations of sepsis and septic shock, including fever, hypotension, acidosis, leukopenia, histopathological evidence of organ injury, and death. In experimental animals, survival is improved when monoclonal (23) or polyclonal (24) antibodies against TNFα are administered before challenge with live *Escherichia coli* or LPS.

Studies in patients (25–28) and experimental animals (29–32) indicate that alterations in myocardial performance are characteristic of sepsis and septic shock. Both left ventricular (LV) systolic dysfunction (depressed ejection fraction) and diastolic dysfunction (decreased chamber compliance) have been documented. Recent data suggest that TNFα is one of the mediators of sepsis-induced cardiac dysfunction. Recombinant human (rh) TNFα induces myocardial depression in dogs (19) and guinea pigs (S. O. Heard, M. W. Perkins, and M. P. Fink, personal communication), and suppresses the positive inotropic effect of isoproteronol in cultured murine fetal heart cells (34).

The purpose of the present study was to rigorously test the hypothesis that rhTNFα impairs LV systolic and diastolic function in chronically instrumented conscious dogs. Alterations in systolic LV function were assessed by analyzing changes in the preload recruitable stroke–work relationship. This relationship is a load-insensitive index of systolic myocardial function that relates increases in LV stroke work to increases in preload (end-diastolic volume or dimension) (35). Changes in the diastolic properties of the left ventricle were assessed by analyzing diastolic transmural pressure–dimension and transmural pressure–strain relationships. A preliminary report of these data has been published (36).

Methods

Surgical preparation. 22 adult mongrel dogs (20–33 kg) were anesthetized with thiopental sodium (25 mg/kg; Abbott Laboratories, North Chicago, IL) and maintained on 1% halothane (Halocarbon Laboratories, Inc., North Augusta, SC) and pancuronium bromide (0.05 mg/

1. *Abbreviations used in this paper:* BEL, ventricular dimension at beginning ejection; C_M, tissue microsphere count; C_R, reference microsphere count; ε, Lagrangian strain; EDL, ventricular dimension at end diastole; EEL, ventricular dimension at end ejection; %ES, fractional ejection shortening of left ventricular minor axis diameter; L, ventricular minor axis dimension; L_0, unstressed ventricular dimension; L_w, x-intercept of the preload recruitable stroke–work relationship; LV, left

ventricular; M_{SW}, slope of the preload recruitable stroke–work relationship; P_A, arterial pressure; P_{LV}, left ventricular intracavitary pressure; P_{PL}, intrapleural pressure; P_{RA}, right atrial pressure; P_{TM}, left ventricular transmural pressure; $\dot{Q}$, cardiac output indexed to body weight; $\dot{Q}_M$, myocardial blood flow; $\dot{Q}_R$, reference blood flow; rhTNFα, recombinant human tumor necrosis factor-α; SVRI, systemic vascular resistance index; SW, stroke work; TNFα, tumor necrosis factor-α.

kg; Quad Pharmaceutical, Inc., Indianapolis, IN). All animals received intravenous cefazolin (500 mg; Eli Lilly & Co., Indianapolis, IN) preoperatively. A left thoracotomy was performed through the fifth intercostal space, and the pericardium was opened and suspended to expose the heart. A pair of ultrasonic dimension transducers (Physiologic Monitoring Systems Group, Durham, NC) were implanted on the LV epicardium adjacent to the anterior and posterior descending coronary arteries to measure the external LV anterior–posterior minor axis diameter (Fig. 1). A pulsed transit time ultrasonic flow probe (model 14348, 12 or 14 mm o.d.; Transonic Systems Inc., Ithaca, NY) was implanted around the pulmonary artery to monitor cardiac output. A silicone rubber catheter (2.6 mm i.d., 4.9 mm o.d.; Dow Corning, Midland, MI) was implanted in the base of the left atrium for injection of microspheres and passage of a catheter-tipped micromanometer to measure LV intracavitary pressure (P_{LV}) during subsequent studies. Another silicone rubber catheter was implanted in the right atrial appendage for measuring right atrial pressure (P_{RA}) and sampling venous blood. A third silicone rubber catheter, closed at its distal end by a compliant silicone rubber balloon (1/100 in thickness), was positioned in the chest at the level of the aortic arch for subsequent passage of a micromanometer to measure intrapleural pressure (P_{PL}). Inflatable silicone rubber occluders (Isis Inc., Minneapolis, MN) were placed around the venae cavae for performing transient vena caval occlusions. The azygous vein was ligated to insure cessation of venous inflow during vena caval occlusions. A fluid-filled polyvinyl chloride catheter was inserted through the left internal mammary artery into the aortic arch to measure arterial pressure (P_A) and to collect arterial blood samples. The electrical leads, catheters, and occluders were all exteriorized dorsal to the thoracotomy incision. A 20 French thoracostomy tube was implanted for postoperative evacuation of fluid and air. The pericardium was left open, and the chest was closed. Postoperatively, all animals received dihydrostreptomycin (0.05 g i.m.) and procaine penicillin (400,000 U i.m.) daily for 6 d (Pfizer Inc., New York). Thoracostomy tubes were removed on the third to fifth postoperative day. The animals were monitored according to the guidelines of the Committee on Animal Research of the University of Massachusetts Medical Center and those prepared by the Committee on Care and Use of Laboratory Animals of the Institute of Laboratory Animal Resources, National Council (DHEW Publication No. [NIH] 85-23, revised 1985).

Instrumentation and data acquisition. Animals were allowed to recover for 7–10 d before being studied. Data were collected with the animals awake and unsedated. P_{LV} and P_{PL} were measured using high fidelity micromanometers (model MPC 500; Millar, Inc., Houston, TX) inserted through the left atrial and pleural catheters, respectively. The micromanometers were zeroed and balanced to atmospheric pressure at 38°C. Pressures in the ascending aorta and right atrium were measured using external transducers (model 800; Bentley Trantec, Elk Grove, IL) connected to the fluid-filled catheters that had been implanted in the aorta and right atrium, respectively. Cardiac rhythm was monitored from lead II of the electrocardiogram.

The ultrasonic dimension transducers were coupled to a sonomicrometer (James W. Davis, Inc., Durham, NC) with a minimal resolution of 0.08 mm, and maximal electronic drift of 0.05 mm/h. The ultrasonic flow probe on the pulmonary artery was coupled to a pulsed transit time flowmeter (Transonic Systems, Inc., Ithaca, NY). Analog signals representing pressures and flow were passed through a series of preamplifiers (Litton Medical Electronics, Inc., Elk Grove, IL) and, together with the signals representing dimension and flow were processed by medium gain amplifiers (James W. Davis, Inc.). The signals were recorded on an eight-channel FM tape recorder (AP Vetter Co., Rebersburg, PA) and simultaneously digitized at a sweep rate of 200 Hz per channel using an analog-to-digital converter (model 1012; ADAC, Woburn, MA) interfaced with a PDP 11/73 computer (Digital Equipment Corp., Maynard, MA).

Experimental Protocol. After the surgical implantation of instrumentation, rectal temperature (T) and body weight were monitored daily. At the time of each study, recordings of heart rate (HR), P_A, P_{RA}, P_{LV}, P_{PL}, LV dimension, and cardiac output were acquired. Arterial blood samples were obtained for determination of pH, PCO_2, and PO_2 (System 1302 blood gas analyzer; Instrumentation Laboratories, Inc., Lexington, MA), and lactate concentration (model 23L lactate analyzer, Yellow Springs Instrument Co., Yellow Springs, OH). Venous blood samples were obtained for determination of plasma concentration of the stable prostacyclin metabolite, 6-keto-$PGF_{1\alpha}$ (37). Signals were then recorded during transient vena caval occlusions, performed over 30 s to bring peak systolic P_{LV} to 30 mmHg.

Baseline data were acquired on the day before rhTNFα administration (day −1) and just before administration (day 0). Animals then received either 100 µg/kg of recombinant human rhTNFα or 100 µg/kg of heat-inactivated rhTNFα (denatured by boiling for 30 min). Recombinant human TNFα (lot EB6011) was supplied by Knoll Pharmaceuticals Inc., Whippany, NJ. Specific activity was 1×10^7 U/mg
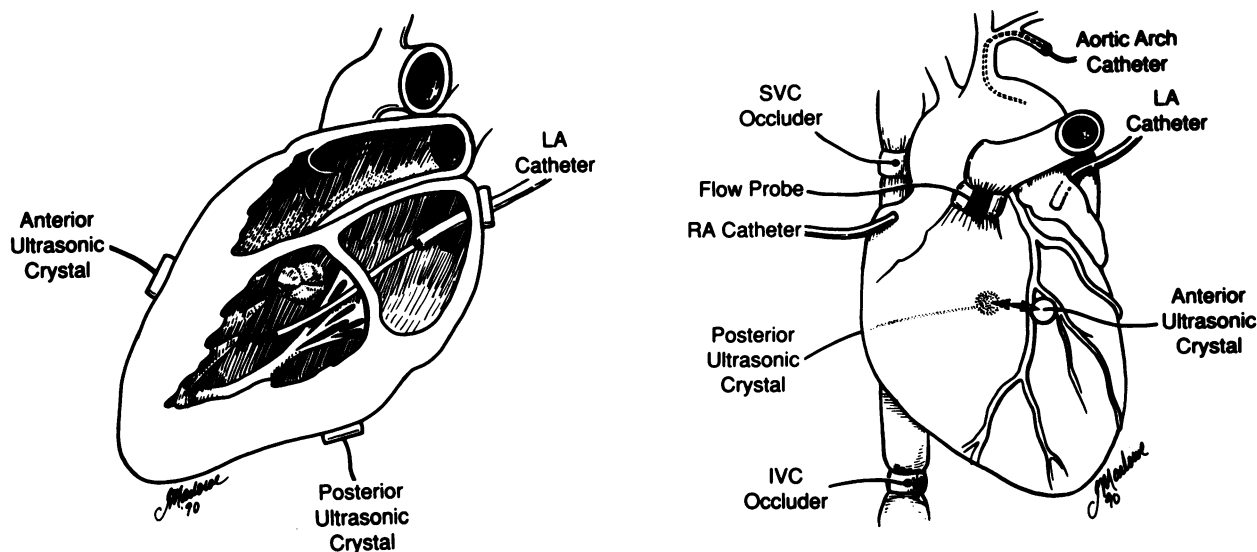
Figure 1. Implantation of instrumentation to monitor cardiac output (pulmonary artery flow probe), external LV anterior–posterior dimension (ultrasonic crystals), aortic and right atrial pressures (fluid-filled catheters). LV pressure was measured with a micromanometer introduced through an implanted left atrial catheter. Inflatable vena caval occluders permitted the adjustment of LV loading during experiments.

protein, and the LPS content was < 0.5 ng/mg protein (manufacturer's data). Individual doses of active rhTNFα or heat-inactivated rhTNFα were reconstituted in 20 ml of saline and administered over 1 h. The administration tubing and syringes were treated with 3 ml of dog plasma before each infusion. Animals received infusions of normal saline before each study to bring end-diastolic P_{LV} to its baseline level. After administration of active or heat-inactivated rhTNFα, data were obtained at 3 and 6 h, and at 1, 2, 3, 5, and 7 d (data from days 3 and 5 are not presented). Myocardial blood flows were determined by injecting color-coded microspheres through the left atrial catheter and sampling blood from the aortic catheter on days 0, 2, and 7. Aerobic and anaerobic blood cultures were obtained from a peripheral vein on days 0, 2, and 7.

At the conclusion of the experiments, the animals were euthanized, and the positions of the ultrasonic dimension transducers were confirmed at autopsy. For the purpose of determining myocardial blood flow, the left ventricle was sectioned into four concentric rings of approximately equal thickness in the plane of the minor axis. The middle two rings were divided into three regions representing the interventricular septum, anterior free wall, and posterolateral free wall. These samples were dissected into epicardial, midmyocardial, and endocardial sections. The epicardial and endocardial thirds (weighing 2–3 g) were then chemically digested, and the number of spheres was determined in each sample (38).

Data analysis. The first derivative of P_{LV} (dP/dt) was calculated as a running five-point orthogonal polynomial approximation from the digital pressure waveform. Diastolic and ejection phases of the cardiac cycle were defined using interactive software. The beginning of diastolic filling was defined as the first zero crossing of the dP/dt waveform following peak negative dP/dt (39). End diastole was defined as the upstroke of the R wave of the electrocardiogram (39). Beginning ejection was defined as the point 10 ms after peak positive dP/dt (39). End ejection was defined as the point 20 ms before peak negative dP/dt (39, 40). Only data from the mid- to end-expiratory phase of the respiratory cycle were considered for analysis to minimize respiratory variation in P_{LV} and LV dimension.

LV transmural pressure (P_{TM}) was calculated as the difference between P_{LV} and P_{PL}: $P_{TM} = P_{LV} - P_{PL}$.

An analogue of LV stroke work (SW) was calculated for individual cardiac cycles as the integral of P_{TM} versus LV anterior–posterior minor axis dimension. Fractional global ejection shortening (%ES) was defined as the change in LV minor axis dimension during the ejection phase of the cardiac cycle normalized to end-diastolic dimension: %ES = (BEL − EEL)/EDL where BEL, EEL, and EDL are beginning ejection, end ejection, and end-diastolic dimension, respectively.

For the purpose of characterizing systolic LV contractility, transient vena caval occlusions were performed to permit the construction of the relationship between SW and LV end-diastolic dimension over a wide range of loading. Data were fit by linear least squares regression to the equation: SW = M_{SW} (EDL − L_W), where M_{SW} and L_W are the derived slope and x-intercept, respectively. Only that portion of the vena caval occlusion in which HR changed by < 10% was considered for analysis.

For the purpose of assessing the passive diastolic compliance of the LV chamber, measured anterior–posterior minor axis dimension was normalized to a Lagrangian strain (ϵ; fractional extension from unstressed dimension): $\epsilon = (L - L_0)/L_0$, where ϵ is the Lagrangian strain of dimension L, and L_0 is the unstressed diastolic dimension, determined at maximal vena caval occlusion, when P_{TM} was equal to 0 mmHg.

Diastolic compliance of the left ventricle was determined by analyzing the relationship between end-diastolic P_{TM} and strain. These data were fit by nonlinear least squares regression to the equation: $P_{TM} = \alpha$ ($e^{\beta\epsilon} - 1$), where α and β are elastic constants determined from the curve fit (41). To compare the pressure–strain relationships of the two experimental groups, the derived α and β values were used to compute strains at LV transmural pressures of 5, 10, and 15, and 20 mmHg. For each group, means and standard deviations of the values of strain at

each pressure were then computed. For the purpose of illustration, exponential forms were also fit to the relationship between end-diastolic P_{TM} and end-diastolic raw dimension (L), again using nonlinear least squares regression: $P_{TM} = \alpha (e^{\beta L} - e^{\beta L_0})$.

Determination of cardiac output and systemic vascular resistance: Cardiac output indexed to body weight ($\dot{Q}$) was computed by dividing the mean pulmonary artery flow measurement by body weight. Systemic vascular resistance index (SVRI) was calculated as: SVRI = ($P_A - P_{RA})/\dot{Q}$.

Assay for plasma levels of 6-keto-PGF$_{1\alpha}$. Venous blood samples were collected into iced-glass tubes containing 100 μg of indomethacin and 10.5 mg of EDTA. Samples were then centrifuged (1,500 g) at 4°C for 15 min. The plasma was collected and stored in polypropylene tubes at −70°C until assayed. Details of the radioimmunoassay for 6-keto-PGF$_{1\alpha}$ (stable hydrolysis product of prostacyclin) have been reported previously (37). The lower limit of sensitivity for the assay is 30 pg/ml. All samples were run in a single assay to obviate interassay variability.

Determination of myocardial blood flow. Microspheres were agitated for 10 min before injection. 7–10 million spheres (15 μm) were injected through the left atrial catheter and flushed with 10 ml of normal saline. A reference arterial blood sample was obtained from the aortic arch at a withdrawal rate of 13.8 ml/min beginning 5 s before injection and continuing for 90 s. Myocardial blood flow, indexed per gram of tissue ($\dot{Q}_M$), was calculated as: $\dot{Q}_M = C_M \cdot \dot{Q}_R/C_R$, where C_M is the microsphere count in the tissue sample, C_R is the number of spheres in the blood reference sample, and $\dot{Q}_R$ is the withdrawal rate of the reference sample.

Statistical analysis. Statistical analyses were performed using commercially available software (SAS Institute, Inc., Cary, NC). For the analyses of myocardial function, the calculated parameters from ten cardiac cycles were averaged. Two-way analysis of variance (ANOVA) with repeated measures was used to compare parameters to their baseline values (at −24 h) over time (within groups) and to compare time-matched parameters between groups (42). When statistically significant differences were identified by ANOVA for group effects or group–time interactions, Tukey's studentized range test for multiple comparisons was used to compare means at individual time points (43). When statistically significant differences within groups over time were observed by ANOVA, single degree of freedom F-tests were used to compare the means at each time with baseline. Bonferonni's correction was utilized to compensate for the increased risk of a type I error with multiple comparisons (44). The null hypothesis was rejected for P < 0.05. Data are presented throughout the tables as means±1 SD.

Results

Disposition of experimental animals (Table I). Of the 22 dogs that underwent implantation of the instrumentation, six were excluded because of technical failures or infectious complications. Of the 16 dogs entered into the study, 10 received active rhTNFα and six received inactivated rhTNFα. Data from 12 of these 16 animals were analyzed; seven that had received active rhTNFα and five controls. Four of the five dogs that died had positive blood cultures and were excluded from the final data analysis. One of the five deaths (active rhTNFα group) occurred at 72 h, immediately after passage of the manometer-tipped catheter into the left ventricle. This death was attributed to an embolic event, and because blood cultures in this animal were negative at 0 and 48 h, data collected before death were analyzed.

Metabolic and respiratory parameters (Table II). There were no significant differences between groups at baseline for these variables: temperature (101.9±0.7 vs. 102.0±0.6°F for control and rhTNFα groups, respectively), arterial pH, Po$_2$, Pco$_2$, and bicarbonate. Controls had slightly higher blood lac-

Table I. Disposition of Experimental Animals

Category	n
Instrumented animals	22
Animals excluded before study	6
Technical failures	2*
Infectious complications	4‡
Animals included for entry into study	16

	Group	
	rhTNFα	Control
Animals studied	10	6
Survivors	6	5
Deaths	4(3§)	1§
Animals included for data analysis	7	5

Deaths occurred at 6 h (2) and 48 h (1) in the active rhTNFα group and 6 h (1) in the controls. One death (72 h) in the active rhTNFα group had negative blood cultures and was included in the final data analysis. * Technical failures (instrumentation failure [2]). ‡ Infectious complications (pneumonia [2], empyema [1], unidentified source [1]). § Animals excluded from the final data analysis because of positive blood cultures (identified organisms: *Enterobacter cloacae* [1]; *Acinetobacter caloaceticus* [1]; *Staphylococcus aureus* [1]; Propinibacteria [1]).

tate concentrations at baseline than did dogs in the rhTNFα group.

Administration of heat-inactivated rhTNFα was associated with minimal changes in temperature (101.7±0.8, 101.6±0.5, 101.2±0.6, 101.3±0.9, and 102.9±0.4°F at 3, 6, 24, 48 h, and 7 d, respectively), arterial blood gases, and arterial concentrations of bicarbonate ion and lactate. Infusion of active rhTNFα elicited a marked febrile response at 3 and 6 h (104.8±1.1 and 103.2±0.1°F, respectively, $P < 0.05$ as compared to baseline,

Table II. Effects of rhTNFα on Arterial pH, PO_2, PCO_2, Bicarbonate, and Lactate Concentration

Time	pH	PO_2	PCO_2	Bicarbonate	Lactate
h		*mmHg*		*meq/liter*	
Control					
−24	7.42±0.02	84±5	37±2	24±1	1.1±0.2
0	7.44±0.03	83±4	36±2	24±1	1.0±0.3
3	7.40±0.02	85±4	37±2	23±2	0.7±0.2
6	7.40±0.03	86±3	37±3	24±2	0.6±0.2*
24	7.42±0.01	84±5	36±3	24±2	0.7±0.2
48	7.41±0.02	92±3*	35±2	23±2	1.0±0.2
168	7.43±0.03	81±6	36±3	24±4	1.2±0.6
rhTNFα					
−24	7.41±0.03	84±6	36±2	23±2	0.7±0.3‡
0	7.42±0.02	85±5	35±2	23±1	0.7±0.1
3	7.40±0.04	78±6*‡	30±3*‡	19±2*‡	1.8±0.1*‡
6	7.28±0.07*‡	82±7	29±3*‡	14±3*‡	2.6±1.3*‡
24	7.31±0.03*‡	83±7	28±6*‡	16±2*‡	0.7±0.2
48	7.36±0.05*‡	85±5‡	31±6*	21±6	0.5±0.1‡
168	7.43±0.02	80±6	34±6	24±2	0.6±0.2

* $P < 0.05$ as compared to baseline. ‡ $P < 0.05$ as compared to control.

102.0±0.6°F and time-matched value in the control group). There were no significant differences in temperature at 24 and 48 h, and 7 d (101.2 ± 0.6, 101.3 ± 0.9, and 102.9 ± 0.4, respectively). Metabolic acidosis was present 6 and 24 h after infusion of the active cytokine. Arterial bicarbonate concentration was decreased at 3, 6, and 24 h; circulating lactate concentrations were increased at 3 and 6 h.

Compared to controls, arterial PO_2 was transiently lower in the rhTNFα group at 3 h. In the active rhTNFα group, arterial PCO_2 was decreased at 3, 6, 24, and 48 h, but recovered to baseline at 72 h.

Hemodynamic variables (Table III). At baseline, hemodynamic variables were comparable in the two groups. Administration of heat-inactivated rhTNFα did not affect HR, peak systolic P_{TM}, end-diastolic P_{TM}, $\bar{P}_A$, dP/dt, $\dot{Q}$, or SVRI. In contrast, infusion of active rhTNFα significantly increased HR, peak systolic P_{TM}, and dP/dt at 3 h. 6 h after the administration of active rhTNFα, HR remained elevated, but peak systolic P_{TM} and dP/dt recovered to baseline values. At 24 h, HR was elevated, whereas peak systolic P_{TM}, dP/dt, $\bar{P}_A$, and SVRI were significantly decreased from baseline. By 48 h, HR, peak systolic P_{TM}, $\bar{P}_A$, and SVRI were all similar to baseline values, although dP/dt was still decreased compared to baseline and compared to the time-matched value in the control group. Except for significantly lower dP/dt in the active rhTNFα group at 72 h (2,436±414 vs. 3,201±318 for rhTNFα and control groups, respectively), there were no further significant differences in hemodynamic variables between the two groups.

In order to maintain end-diastolic P_{LV} at its baseline value during the course of each study, animals receiving active rhTNFα required resuscitation with a larger ($P < 0.05$) volume of normal saline as compared to baseline and time-matched control values at 3, 6, and 24 h (17±10 vs. 18±18, 2±3 vs. 34±14, 2±4 vs. 39±20, 4±6 vs. 65±27, 12±12 vs. 24±22, and 9±11 vs. 17±16 ml/kg for control and rhTNFα groups at −24, 3, 6, 24, 48 h, and 7 d, respectively.

Left ventricular function (Table IV). There were no significant differences between the two groups in the baseline indices of systolic myocardial contractile function (SW, %ES, or slope and intercept of the preload recruitable stroke–work relationship). LV stroke work, %ES, and the slope and x-intercept of the preload recruitable stroke–work relationship were stable in animals infused with heat-inactivated rhTNFα (Figs. 2 and 3).

At 3 and 6 h after the administration of active rhTNFα, there was no evidence of systolic myocardial dysfunction as assessed by analysis of SW and the slope and intercept of the preload recruitable stroke work relationship. Fractional ejection shortening was significantly smaller than in the controls at 3, 6, 24, 48, and 72 h.

At 24 h, both SW and %ES were decreased significantly from baseline. These changes were accompanied by a decrease in the slope and a rightward shift (increase in x-intercept) of the preload recruitable stroke–work relationship, so that at any given LV end-diastolic dimension, LV stroke work was significantly decreased (Fig. 3). By 48 h, SW and the slope and intercept of the preload recruitable stroke–work relationship were not significantly different from baseline, although the x-intercept remained significantly different from the controls until 72 h.

The diastolic relationships between LV end-diastolic P_{TM} and either LV end-diastolic dimension (Fig. 4) or normalized

Table III. Effects of rhTNFα on Hemodynamic Indexes

Time	Heart rate	Peak systolic LV transmural pressure	End-diastolic LV transmural pressure	Mean arterial pressure	dP/dt	Cardiac index	Systemic vascular resistance index
h	$beats \cdot min^{-1}$		$mmHg$		$mmHg \cdot s^{-1}$	$liters \cdot min^{-1} \cdot kg^{-1}$	$mmHg \cdot min \cdot kg \cdot liter^{-1}$
Control							
−24	102±13	126±4	13.5±1.2	111±4	3,112±473	0.14±0.02	868±284
0	96±15	128±9	14.1±2.5	110±8	3,011±403	0.13±0.02	858±277
3	95±18	127±9	13.4±3.2	111±6	3,126±433	0.13±0.02	837±139
6	95±16	123±6	11.2±2.7	108±4	3,227±367	0.13±0.03	819±228
24	92±18	126±5	12.1±3.1	110±3	3,037±366	0.12±0.02	946±252
48	96±14	124±8	11.2±1.7	109±7	3,094±375	0.14±0.04	842±382
168	95±23	132±4	13.9±3.3	117±4	3,275±124	0.13±0.03	947±294
rhTNFα							
−24	100±16	133±8	13.5±5.5	115±7	2,803±290	0.11±0.01	934±58
0	99±17	136±10	13.6±5.2	114±11	2,971±319	0.12±0.01	920±119
3	117±25*	145±9*‡	9.3±4.9	117±9	3,280±715*	0.13±0.03	969±312
6	121±15*‡	132±8	10.8±5.1	108±13	2,984±597	0.13±0.02	879±122
24	133±19*‡	112±16*	14.6±4.6	95±17*	1,789±454*‡	0.12±0.01	674±124*
48	110±15	127±8	16.1±5.7	113±7	1,972±310*‡	0.10±0.01	1,091±190
168	105±7	139±6	13.4±4.6	116±6	3,165±282	0.14±0.03	853±222

* $P < 0.05$ as compared to baseline. ‡ $P < 0.05$ as compared to control group.

LV dimension (strain) (Figs. 5 and 6) were not significantly different at baseline between the control and active rhTNFα groups. Administration of heat-inactivated rhTNFα had no effect on these relationships (Fig. 4) or on unstressed LV dimension (Table IV).

Administration of active rhTNFα elicited significant changes in the diastolic relationships of the left ventricle that were initially manifested 24 h after infusion of the cytokine. These changes were characterized by a rightward shift of the LV end-diastolic P_{TM}–dimension relationship (Fig. 4) and an increase in L_0 (Table IV). On the basis of the increase in L_0, there was a significant leftward shift in the end-diastolic P_{TM}–strain relationship (Figs. 5 and 6), with significant differences from the controls evident at 24 and 48 h. The leftward shift of the end-diastolic P_{TM}–strain relationship is consistent with a decrease in LV chamber compliance. By 72 h, the end-diastolic P_{TM}–strain relationship returned to baseline (Figs. 5 and 6).

Myocardial blood flow (Table V). There were no significant differences in baseline subepicardial or subendocardial $\dot{Q}_M$ between control and active rhTNFα groups. After the ad-

Table IV. Effects of rhTNFα on Fractional Ejection Shortening, LV Stroke Work, Intercept of the Preload Recruitable Stroke-Work Relationship, L_0, Slope of the Preload Recruitable Stroke-Work Relationship, and LV End-Diastolic Dimension

Time	LV stroke work	LV fractional ejection shortening	Slope of the preload recruitable stroke-work relationship	Intercept of the preload recruitable stroke-work relationship	Unstressed LV dimension	LV end-diastolic dimension
h	$ergs \cdot cm^{-2}$	%	$ergs \cdot cm^{-2} \cdot mm^{-1}$		mm	
Control						
−24	77,230±15,110	9.1±1.0	8,698±2,341	44.3±2.2	42.6±2.1	54.7±4.0
0	75,415±12,143	8.9±0.7	8,141±1,894	44.2±2.1	42.8±2.1	53.9±3.5
3	75,665±11,864	8.9±0.9	7,861±1,500	43.3±2.8	42.0±2.6	53.8±3.7
6	76,753±14,000	9.2±1.0	8,417±1,992	44.2±2.4	41.7±3.1	53.7±3.8
24	74,020±6,696	8.7±0.7	7,973±1,486	44.0±2.4	42.3±1.8	53.7±3.5
48	75,967±8,197	9.2±1.3	8,117±1,635	43.7±2.3	41.7±3.1	53.6±3.9
168	76,353±6,688	8.9±1.0	8,379±1,896	43.7±2.3	41.4±2.1	52.4±2.4
rhTNFα						
−24	77,995±14,570	7.6±1.4	7,718±1,735	47.4±3.9	44.8±4.8	58.0±3.8
0	84,230±16,800	7.9±1.3	7,800±1,931	47.3±3.9	44.5±5.1	58.3±3.9
3	75,797±21,311	6.6±1.6‡	8,430±2,193	47.9±3.5	45.3±4.8	57.2±4.4
6	67,281±17,841	6.7±1.6‡	7,586±902	48.4±4.1	44.9±4.2	57.6±4.3
24	53,074±21,118*‡	6.3±1.1*‡	5,886±2,356*‡	49.9±4.1*‡	48.4±4.6*‡	59.2±4.8‡
48	64,351±14,430	6.5±0.8‡	6,619±2,321	49.7±4.6*‡	47.5±6.1	59.8±4.8‡
168	85,863±21,386	7.7±1.6	8,877±2,928	47.7±6.2	45.1±8.2	57.6±6.4

* $P < 0.05$ as compared to baseline. ‡ $P < 0.05$ as compared to control group.

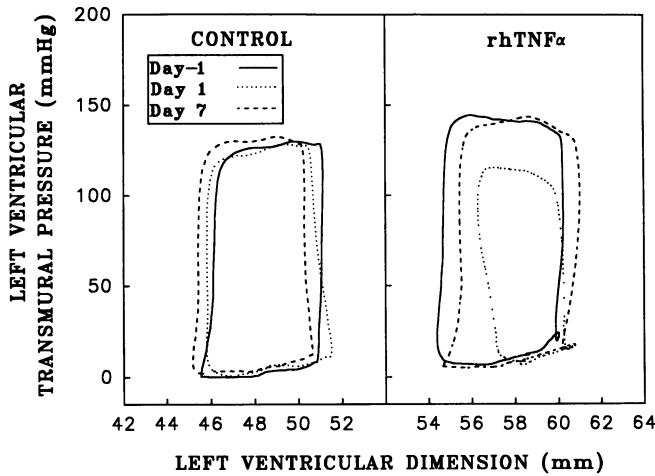*Figure 2.* Transmural pressure–minor axis dimension loops for individual cardiac cycles. 1 d after the infusion of rhTNFα, ejection shortening and peak-systolic P_{TM} were reduced despite preservation of preload (end-diastolic dimension). By 7 d, ejection shortening and peak-systolic pressure were restored.

Figure 4. End-diastolic relationships between P_{TM} and LV dimension in representative animals, 1 d after active infusion of rhTNFα the P_{TM}-dimension relationship was displaced to the right, with larger dimension at any given P_{TM}, including $P_{TM} = 0$ mmHg. The position of this relationship was restored at 7 d.

ministration of heat-inactivated or active rhTNFα, there were no significant changes in subepicardial or subendocardial blood flow.

6-keto-PGF$_{1\alpha}$ (Table VI). There were no significant differences between the two groups in baseline venous plasma levels of 6-keto-PGF$_{1\alpha}$. Administration of active rhTNFα elicited significant increases in 6-keto-PGF$_{1\alpha}$ at 3 and 6 h. By 24 h, plasma levels of 6-keto-PGF$_{1\alpha}$ returned to baseline.

Discussion

Effect of rhTNFα on LV function. Infusion of rhTNFα resulted in reversible systolic and diastolic LV dysfunction in chronically instrumented, conscious dogs. The onset of myocardial dysfunction was not observed until 24 h after the infusion of rhTNFα. At this time, HR was significantly increased, and
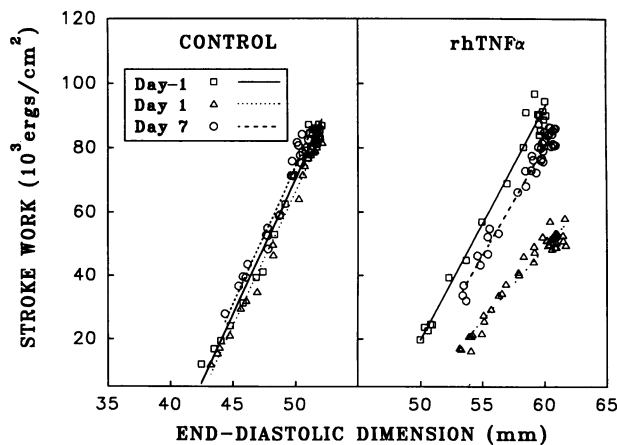
peak systolic P_{TM}, $\bar{P}_A$, and SVRI were significantly decreased. LV end-diastolic P_{TM} (preload) was maintained at baseline levels by infusing large volumes of normal saline. Despite the presence of myocardial dysfunction and decreased stroke volume, $\dot{Q}$ was well maintained. By 72 h, LV function recovered to baseline in all animals.

A hyperdynamic circulatory state with concomitant depression of myocardial function similar to that observed in this study has been described in studies of sepsis and septic shock (24, 26–31). Thus, our data suggest that rhTNFα is capable of eliciting the pattern of hemodynamic derangements and myocardial dysfunction characteristic of the sepsis syndrome. Our findings are therefore consistent with the hypothesis that TNFα is a mediator of some of the circulatory and cardiac manifestations of sepsis and septic shock. In the present study, systolic myocardial dysfunction was evidenced by a rightward shift and

Figure 3. LV end-diastolic dimension–stroke work relationships in representative animals. 1 d after infusion of active rhTNFα, the end-diastolic dimension–stroke work relationship was shifted to the right with a small decrease in slope. The position and slope of this relationship were nearly restored at 7 d.
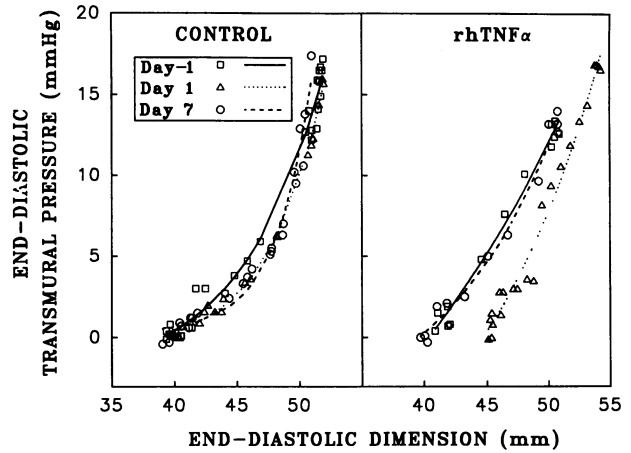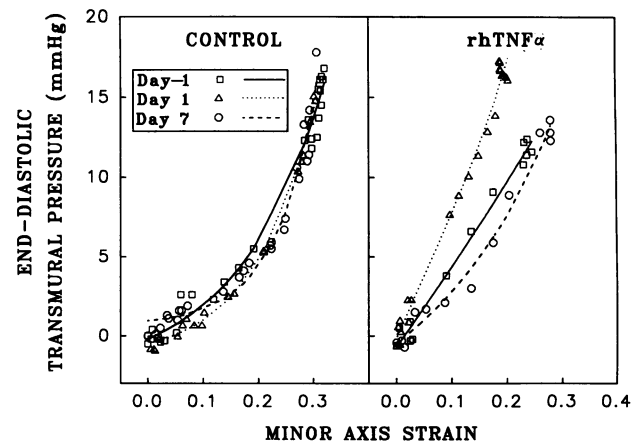

Figure 5. End-diastolic relationships between P_{TM} and normalized LV dimension (strain) in representative animals. 1 d after the infusion of active rhTNFα, the P_{TM}-strain relationship was displaced to the left with higher P_{TM} at any given strain. By 7 d, the P_{TM}-strain relationship had returned close to its baseline position.
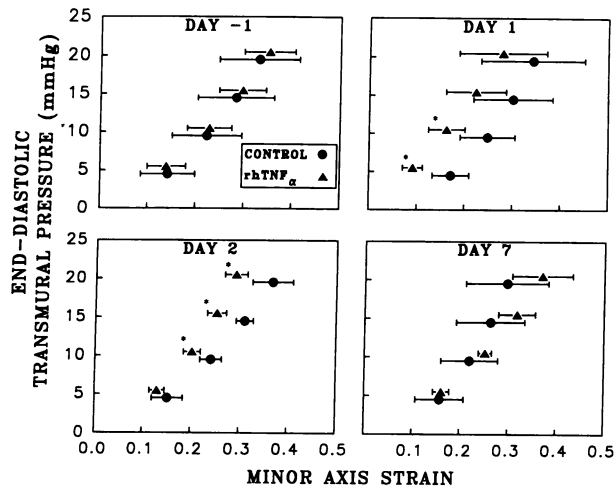
Figure 6. Means of end-diastolic P_{TM}-strain data for the two groups of dogs. The P_{TM}-strain relationship of the group that received active rhTNFα was displaced to the left of the P_{TM}-strain relationship of the control animals on day 1, with significantly smaller strains at 5 and 10 mmHg of pressure. On day 2, strains in the active rhTNFα group were significantly smaller than strains in the control group at 10, 15, and 20 mmHg.

Table VI. Effects of rhTNFα on Plasma Levels of 6-keto-PGF$_{1\alpha}$

Time	6-keto-PGF$_{1\alpha}$
h	*pg/ml*
Control	
−24	97±167
0	113±191
3	102±183
6	71±129
24	71±118
48	81±135
168	86±173
rhTNFα	
−24	57±68
0	31±57
3	548±299*‡
6	1,110±258*‡
24	84±101
48	70±107
168	53±81

* $P < 0.05$ as compared to baseline. ‡ $P < 0.05$ as compared to control group.

depression of the slope of the preload recruitable stroke work relationship, so that at any given LV preload (end-diastolic dimension), there was a significant reduction in the analogue of LV stroke work. The reduction in stroke work was due to both a decrease in fractional shortening of the minor axis dimension during the ejection phase of systole, and a decrease in peak systolic LV pressure. Myocardial depression was sufficient to decrease ejection shortening despite a concomitant reduction in SVRI (a proxy for LV afterload) and maintenance of baseline levels of preload (end-diastolic P_{TM} and EDL). Fractional ejection shortening was depressed at 3 and 6 h, possibly owing to either increases in afterload, decreases in preload, or decreases in contractility that were not detectable in our model. Systolic myocardial dysfunction at 24 h also was evidenced by a significant reduction in the maximal rate of rise of LV pressure during isovolumic systole (dP/dt). This parameter is sensitive to loading conditions, however, and may have been influenced by the decrease in peak systolic P_{TM}.

The most important finding of this study was the observation that infusion of rhTNFα caused significant diastolic dysfunction of the left ventricle characterized by these features: (*a*)

Table V. Effects of rhTNFα on Myocardial Blood Flow

Time	Subendocardial flow	Subepicardial flow
h	$ml \cdot min^{-1} \cdot g^{-1}$	
Control		
0	1.14±0.20	0.96±0.08
48	1.07±0.32	0.93±0.30
168	1.10±0.54	0.94±0.50
rhTNFα		
0	1.09±0.81	0.83±0.44
48	0.94±0.31	0.72±0.15
168	0.89±0.61	0.75±0.41

a significant increase in LV unstressed dimension, L_0, (i.e., diastolic creep); (*b*) a rightward shift of the LV end-diastolic P_{TM}-dimension relationship generated during vena caval occlusions; and (*c*) a leftward shift of the LV end-diastolic P_{TM}-strain relationship. Recent experimental studies have demonstrated LV dilatation 48 h after administration of rhTNFα (19). Whether this change represents physiologic LV dilatation or a change in LV chamber compliance was investigated in our model by analyzing changes in unstressed dimension and strain (fractional extension from unstressed dimension). 24 and 48 h after the infusion of rhTNFα, there was an increase in unstressed dimension (creep) and a significant leftward shift of the LV end-diastolic P_{TM}-strain relationship, so that at any given end-diastolic strain, there was a greater LV end-diastolic P_{TM}. The findings suggest that the administration of rhTNFα alters the diastolic elastic properties of the LV wall, resulting in a significant reduction in LV chamber compliance. Chamber compliance can also be altered by changes in external constraints to filling (pressure and volume loading of the right ventricle or increases in intrapericardial pressure [45]), however, there was no evidence for these mechanisms in the present study. Specifically, right atrial filling pressures were not significantly different over time or between control or rhTNFα groups (data not shown). The finding that diastolic function is impaired, suggests that the LV dilatation noted by us and by Natanson et al. (19) is not simply dilatation of the left ventricle along its normal pressure–volume relationship to compensate for systolic dysfunction.

Stahl and colleagues (31) demonstrated diastolic creep with decreased LV diastolic compliance during sepsis induced by cecal ligation and puncture in dogs. Because the changes in diastolic LV function elicited by rhTNFα are similar to those observed in this canine model of sepsis, it is plausible to hypothesize that TNFα is a mediator of sepsis-induced alterations in the diastolic mechanical properties of the myocardium.

During the course of several days, there are three mechanisms that could explain the rhTNFα-induced elongation of the external diameter of the left ventricle at zero stress: (*a*) elongation of myocardial fibers, (*b*) rearrangement of the interstitial matrix, and (*c*) formation of myocardial edema. Studies examining cardiac enlargement during models of ischemic injury and hemodynamic overload have demonstrated that increases in ventricular dimension can in part be accounted for by changes in fiber length (reflected by changes in sarcomere length [46–48]), by slippage and realignment of the fibers (orderly rearrangement of the interstitial matrix [48, 49]), and by disruption of the interstitial matrix (48, 50). Although elongation of sarcomere length and slippage between fiber layers probably occurs during ventricular expansion related to physiologic increases in preload, the elongation of dimension at a fixed stress (zero) suggests a change in fiber length or fiber arrangement that is not immediately reversible by physiologic restoring forces. In the case of rhTNFα-induced diastolic dysfunction, it is unknown whether elongation of unstressed dimension represents injury to the myocardial fibers and contractile proteins or disruption of the interstitial matrix. In the setting of reversible contractile dysfunction associated with myocardial stunning, extensive damage to the interstitial matrix has been demonstrated (50). The interstitial injury accompanying myocardial stunning is detectable within 3–4 h, and occurs in the absence of a local inflammatory response or myocardial necrosis. Invoking damage to the interstitial matrix as the cause of the ventricular enlargement observed in the present study would be compatible with the reversibility of the creep induced by rhTNFα, but would not in itself explain the delayed onset of creep.

The measurement of an external LV diameter with epicardial dimension transducers includes the measurement of two wall thicknesses. If infusion of rhTNFα elicited the formation of myocardial edema with a concomitant increase in wall thickness, an increase in the external anterior–posterior minor axis dimension could have occurred in our experiments without a true increase in the internal diameter and volume of the left ventricle. We did not measure water content of the myocardium or changes in wall thickness to exclude this possibility. However, the large mass of edema necessary to account for the observed change in L_0 would likely have caused far more severe systolic dysfunction. For an extension of L_0 from 4.5 to 4.8 cm to occur on the basis of an increase in wall thickness only, enough edema would have to be present in an equatorial LV ring to increase its mass by $\sim$ 20%. Previous studies have demonstrated that, with a comparable increase in LV mass owing to edema, cardiac output is reduced $\sim$ 50% at fixed preload (left atrial pressure = 15 mmHg) (51).

Whether TNFα-induced myocardial injury is primarily to myocytes or to the interstitial matrix, the intermediate mechanisms underlying this injury remain unknown. Both direct effects of TNFα on the myocardium or effects by secondary mediators seem plausible. It is unlikely that myocardial depression in our study was the result of rhTNFα-induced systemic metabolic abnormalities. At the time of maximum myocardial depression (24 h), animals were only mildly acidemic (pH 7.31±0.03). It is unlikely that this level of acidosis can account for the observed degree of systolic dysfunction myocardial depression, since at 6 h, when systemic acidosis was more severe, there was no evidence of myocardial depression. Ventricular dysfunction also cannot be attributed to changes in subendocar-

dial or subepicardial blood flow. Both systolic and diastolic dysfunction were evident at 48 h, when $\dot{Q}_M$ was not significantly less than baseline.

Myocardial injury induced by TNFα may depend upon the recruitment and activation of neutrophils. This hypothesis is consistent with these findings: (*a*) TNFα enhances margination and infiltration of neutrophils through endothelium (52, 53); (*b*) TNFα promotes adhesion of neutrophils to cardiac myocytes (54); and (*c*) neutrophils participate in ischemic myocardial injuries that result in both cell death and reversible contractile dysfunction (55–60). There is also evidence that TNFα promotes systemic and local release of secondary mediators from white blood cells (61–65) that could potentially compromise myocardial contractile function (66–70). The finding in this study that the onset of ventricular dysfunction occurs 6–24 h after administration of rhTNFα, could be explained by neutrophil activation and subsequent infiltration into the myocardium with systemic and local release of mediators over a period of several hours.

Recent in vitro studies have described a direct effect of TNFα on the sympathomimetic stimulation of myocardial contractile function. Myocytes exposed to TNFα for 72 h demonstrate a decrease in isoproterenol-stimulated augmentation of contractile activity and production of cAMP (34). These effects occur without a change in the density or affinity of β-adrenergic receptors. The response to forskolin, an inhibitor of adenylate cyclase, is not affected by exposure to TNFα (34). These data suggest that myocardial cells express receptors for TNFα, which when activated, elicit derangements in the β receptor—regulatory GTP binding protein—adenylate cyclase transduction system (71).

Effects of rhTNFα on hemodynamics, prostacyclin release, and arterial oxygenation. Consistent with previous reports by others (22), we observed a marked increase in circulating levels of 6-keto-$PGF_{1\alpha}$ after infusion of rhTNFα. We measured levels of this prostanoid as an internal check to document that the cytokine was indeed active. Also consistent with previously published results (21, 22) was our observation that infusion of rhTNFα elicited fever and arterial hypoxemia, and decreased SVRI during the early (3–24 h) period after infusion.

Critique of experimental methods. The assessment of systolic and diastolic myocardial function in this study relied upon the analysis of a single external ventricular dimension (anterior–posterior axis diameter). Changes in this linear dimension have been substituted for changes in LV volume. Systolic stroke work is a pressure–volume integral rather than a pressure–dimension integral, and a more complete description of LV chamber compliance requires analysis of the diastolic pressure–volume relationship, rather than a pressure–diameter relationship. However, Rankin et al. (72) have demonstrated in a similar experimental preparation that changes in the anterior–posterior minor axis dimension during the cardiac cycle are highly correlated with changes in LV volume. We have validated under baseline conditions that changes in minor axis dimension during the ejection phase are highly correlated with changes in stroke volume, measured independently with the pulmonary artery flow probe used in this study (F. D. Pagani, unpublished observations).

The present study leaves some uncertainty in the time of onset of mechanical dysfunction of the left ventricle. Because no data were collected between 6 h and 24 h, the true onset of LV dysfunction may have occurred between these two time

points. Latent LV contractile dysfunction at earlier time points may have been masked by adrenergic stimulation. Furthermore, the statistical power of this study was limited by the availability of only a seven- animal × five-animal matrix of data for final analysis.

Finally, rather than obtaining tissue from ventricles for histologic and biochemical analysis at the time of their maximal dysfunction (24–48 h), we elected to document the reversibility of ventricular dysfunction and the time course of recovery. Future studies in which tissue is harvested 24–48 h after the administration of rhTNFα will therefore be necessary to elucidate the histologic and biochemical substrates of the myocardial injury.

Acknowledgments

References

1. Waage, A., T. Espevik, and J. Lamvik. 1986. Detection of tumour necrosis factor-like cytotoxicity in serum from patients with septicaemia but not from untreated cancer patients. Scand. J. Immunol. 24:739–743.

2. Waage, A., T. Espevik, and A. Halstensen. 1987. Association between tumour necrosis factor in serum and fatal outcome in patients with meningococcal disease. Lancet. i:355–357.

3. Michie, H. R., K. R. Manogue, D. R. Spriggs, A. Revhaug, S. O'Dwyer, C. A. Dinarello, A. Cerami, S. M. Wolff, and D. G. Wilmore. 1988. Detection of circulating tumor necrosis factor after endotoxin administration. N. Engl. J. Med. 318:1481–1486.

4. Mathison, J. C., E. Wolfson, and R. J. Ulevitch. 1988. Participation of tumor necrosis factor in the mediation of gram negative bacterial lipopolysaccharide-induced injury in rabbits. J. Clin. Invest. 81:1925–1937.

5. Evans, G. F., Y. M. Snyder, L. D. Butler, and S. H. Zuckerman. 1989. Differential expression of interleukin-1 and tumor necrosis factor in murine septic shock models. Circ. Shock. 29:279–290.

6. Hesse, D. G., K. J. Tracey, Y. Fong, K. R. Manogue, M. A. Palladino, Jr., A. Cerami, and G. T. Shires. 1988. Cytokine appearance in human endotoxemia and primate bacteremia. Surg. Gynecol. Obstet. 166:147–153.

7. Kiener, P. A., F. Marek, G. Rodgers, L. Pin-Fang, G. Warr, G., and J. Desiderio. 1988. Induction of tumor necrosis factor, IFN-gamma, and acute lethality in mice by toxic and non-toxic forms of lipid A. J. Immunol. 141:870–874.

8. Blick, M., S. A. Sherwin, M. Rosenblum, and J. Gutterman. 1987. Phase I study of recombinant tumor necrosis factor in cancer patients. Cancer. Res. 47:2986–2989.

9. Spriggs, D. R., M. L. Sherman, H. Michie, K. A. Arthur, K. Imamura, D. Wilmore, E. Frei III., and W. K. Kufe. 1988. Recombinant human tumor necrosis factor administered as a 24-hour intravenous infusion: a phase I and pharmacologic study. J. Natl. Cancer. Inst. 80:1039–1044.

10. Remick, D. G., R. G. Kunkel, J. W. Larrick, and S. L. Kunkel. 1987. Acute in vivo effects of human recombinant tumor necrosis factor. Lab. Invest. 56:583–590.

11. Rothstein, J. L., and H. Schreiber. 1988. Synergy between tumor necrosis factor and bacterial products causes hemorrhagic necrosis and lethal shock in normal mice. Proc. Natl. Acad. Sci. USA. 85:607–611.

12. Gaskill, H. V. 1988. Continuous infusion of tumor necrosis factor: mechanisms of toxicity in the rat. J. Surg. Res. 44:664–671.

13. Kettlehut, I. C., W. Fiers, and A. L. Goldberg. 1987. The toxic effects of tumor necrosis factor in vivo and their prevention by cyclooxygenase inhibitors. Proc. Natl. Acad. Sci. USA. 84:4273–4277.

14. Tracey, K. J., B. Beutler, S. F. Lowry, J. Merryweather, S. Wolpe, I. W. Milsark, R. J. Hariri, T. J. Fahey, A. Zentella, J. D. Albert, et al. 1986. Shock and tissue injury induced by recombinant human cachectin. Science (Wash. DC). 234:470–474.

15. Schirmer, W. J., J. M. Schirmer, and D. E. Fry. 1989. Recombinant

16. Turner, C. R., K. M. Esser, E. B. Wheeldon, Slivjak, and E. F. Smith. 1989. Cardiovascular and pulmonary effects of human recombinant tumor necrosis factor in the conscious rat. Circ. Shock. 28:369–384.

17. Okusawa, S., J. A. Gelfand, T. Ikejima, R. J. Connolly, and C. A. Dinarello. 1988. Interleukin 1 induces a shock-like state in rabbits. J. Clin. Invest. 81:1162–1172.

18. Evans, D. A., D. O. Jacobs, A. Revhaug, and D. W. Wilmore. 1989. The effects of tumor necrosis factor and their selective inhibition by ibuprofen. Ann. Surg. 209:312–321.

19. Natanson, C., P. W. Eichenholz, R. L. Danner, P. Q. Eichacker, W. D. Hoffman, G. C. Kuo, S. M. Banks, T. J. MacVittie, and J. E. Parrillo. 1989. Endotoxin and tumor necrosis factor challenges in dogs simulate the cardiovascular profile of human septic shock. J. Exp. Med. 169:823–832.

20. Tracey, K. J., S. F. Lowry, T. J. Fahey III, J. D. Albert, Y. Fong, D. Hesse, B. Bentler, K. R. Manaque, S. Calvano, H. Wei, et al. 1987. Cachectin/tumor necrosis factor induces lethal shock and stress hormone responses in the dog. Surg. Gynecol. Obstet. 164:415–422.

21. Johnson, J., B. Meyrick, G. Jesmok, and K. L. Brigham. 1989. Human recombinant tumor necrosis factor alpha infusion mimics endotoxemia in awake sheep. J. Appl. Physiol. 66:1448–1454.

22. Kreil, E. A., E. Greene, C. Fitzgibbon, D. R. Robinson, and W. M. Zapol. 1989. Effects of recombinant human tumor necrosis factor alpha, lymphotoxin, and E. coli lipopolysaccharide on hemodynamics, lung microvascular permeability, and eicosanoid synthesis in anesthetized sheep. Circ. Res. 65:502–514.

23. Tracey, K. J., Y. Fong, D. G. Hesse, K. R. Manogue, A. T. Lee, G. C. Kuo, S. F. Lowry, and A. C. Cerami. 1987. Anti-cachectin/TNF monoclonal antibodies prevent septic shock during lethal bacteraemia. Nature (Lond.). 330:662–664.

24. Beutler, B., I. W. Milsark, and A. C. Cerami. 1985. Passive immunization against cachectin/tumor necrosis factor protects mice from lethal effect of endotoxin. Science (Wash. DC). 229:869–871.

25. Ellrodt, A. G., M. S. Riedinger, A. Kimchi, D. S. Berman, J. Maddahi, H. J. C. Swan, and G. H. Murata. 1985. Left ventricular performance in septic shock: reversible segmental and global abnormalities. Am. Heart J. 110:402–408.

26. MacLean, L. D., W. G. Mulligan, A. P. H. McLean, and J. H. Duff. 1967. Patterns of septic shock in man: a detailed study of 56 patients. Ann. Surg. 166:543–562.

27. Natanson, C., R. L. Danner, R. R. Elin, J. M. Hosseini, K. W. Peart, S. M. Banks, T. J. MacVittie, R. I. Walker, and J. E. Parrillo. 1989. Role of endotoxemia in cardiovascular dysfunction and mortality. J. Clin. Invest. 83:243–251.

28. Parker, M. M., J. H. Shelhamer, S. L. Bacharach, M. V. Green, C. Natanson, T. M. Frederick, B. A. Damske, and J. E. Parrillo. 1984. Profound but reversible myocardial depression in patients with septic shock. Ann. Intern. Med. 100:483–490.

29. Natanson, C., R. L. Danner, M. P. Fink, T. J. MacVittie, R. I. Walker, J. J. Conklin, and J. E. Parrillo. 1988. Cardiovascular performance with E. coli challenges in a canine model of human sepsis. Am. J. Physiol. 254:H558–H569.

30. Natanson, C., M. P. Fink, H. K. Ballantyne, H. K., T. J. MacVittie, J. J. Conklin, and J. E. Parrillo. 1986. Gram-negative bacteremia produces both severe systolic and diastolic cardiac dysfunction in a canine model that stimulates human septic shock. J. Clin. Invest. 78:259–270.

31. Stahl, T. J., P. B. Alden, W. S. Ring, R. C. Madoff, and F. B. Cerra. 1990. Sepsis-induced diastolic dysfunction in chronic canine peritonitis. Am. J. Physiol. 258:H625–H633.

32. Pasque, M. K., P. Van Trigt, G. L. Pellom, B. M. Freedman, and A. S. Wechsler. 1988. Assessment of the intrinsic contractile status of the heart during sepsis by myocardial pressure-dimension analysis. Ann. Surg. 208:110–117.

33. Reference removed in proof.

34. Gulick, T., M. K. Chung, S. J. Pieper, L. G. Lange, and G. F. Schreiner. 1989. Interleukin-1 and tumor necrosis factor inhibit cardiac myocyte β-adrenergic responsiveness. Proc. Natl. Acad. Sci. USA. 86:6753–6757.

35. Glower, D. D., J. A. Spratt, N. D. Snow, J. S. Kabas, J. W. Davis, C. O. Olsen, G. S. Tyson, D. C. Sabiston, and J. S. Rankin. 1985. Linearity of the Frank-Starling relationship in intact heart: the concept of preload recruitable stroke work. Circulation. 71:994–1009.

36. Pagani, F. D., L. S. Baker, M. A. Knox, H. Cheng, M. P. Fink, and M. S. Visner. 1990. Tumor necrosis factor alpha causes diastolic creep and reversible left ventricular systolic dysfunction in conscious dogs. Surg. Forum. 41:40–42. (Abstr.)

37. Fink, M. P., W. M. Gardiner, R. Roethel, and J. R. Fletcher. 1985. Plasma levels of 6-keto-PGF₁α but not TxB₂ increase in rats with peritonitis due to cecal ligation. Circ. Shock. 16:297–305.

38. Hale, S. L., K. J. Alker, and R. A. Kloner. 1988. Evaluation of nonradioactive, colored microspheres for measurement of regional myocardial blood flow in dogs. Circulation. 78:428–434.

39. Glower, D. D., J. A. Spratt, J. S. Kabas, J. W. Davis, and J. S. Rankin. 1988. Quantification of regional myocardial dysfunction after acute ischemic injury. Am. J. Physiol. 255:H85–H93.

40. Abel, F. L. 1981. Maximum negative dP/dt as an indicator of end systole. *Am. J. Physiol.* 240:H676–H682.

41. Rankin, J. S., C. E. Arentzen, P. A. McHale, D. Ling, and R. W. Anderson. 1974. Viscoelastic properties of the diastolic left ventricle in the conscious dog. *Circ. Res.* 41:37–45.

42. Dunn, O. J., and V. A. Clark. 1987. Applied Statistics: Analysis of Variance and Regression. John Wiley & Sons, Inc., New York. 236 pp.

43. Box, G. E. P., W. G. Hunter, and J. S. Hunter. 1978. Statistics for Experiments, An Introduction to Design, Data Analysis and Model Building. John Wiley & Sons, Inc., New York. 204 pp.

44. Milliken, G. A., and D. E. Johnson. 1984. Analysis of Messy Data. Lifetime Learning Publications, Belmont, CA. 33 pp.

45. Glantz, S. A., and W. W. Parmley. 1978. Factors which affect the diastolic pressure-volume curve. *Circ. Res.* 42:171–180.

46. Zhao, M., R. Forman, E. H. Sonnenblick. 1989. Pressure-sarcomere length relationship in the stunned myocardium. *Circulation.* 80:II-97.

47. Glower, D. D., J. Schaper, J. S. Kabas, H. M. Hoffmeister, W. Schaper, J. A. Spratt, J. W. Davis, and J. S. Rankin. 1987. Relation between reversal of diastolic creep and recovery of systolic function after ischemic myocardial injury in conscious dogs. *Circ. Res.* 60:850–860.

48. Factor, S. M., M. Flomenbaum, M. Zhao, C. Eng, and T. F. Robinson. 1988. The effects of acutely increased ventricular cavity pressure on intrinsic myocardial connective tissue. *J. Am. Coll. Cardiol.* 1582–1589.

49. Weisman, H. F., D. E. Bush, J. A. Mannisi, M. L. Weisfeldt, and B. Healy. 1988. Cellular mechanisms of myocardial infarct expansion. *Circulation.* 78:186–201.

50. Zhao, M., H. Zhang, T. F. Robinson, S. M. Factor, and E. H. Sonnenblick. 1987. Profound Structural alterations of the extracellular collagen matrix in post-ischemic dysfunctional ("stunned") but viable myocardium. *J. Am. Coll. Cardiol.* 6:1322–1334.

51. Laine, G. A., and S. J. Allen. 1991. Left ventricular myocardium edema. Lymph flow, interstitial fibrosis, and cardiac function. *Circ. Res.* 68:1713–1721.

52. Pohlman, T. H., K. A. Stanness, P. G. Beatty, H. D. Ochs, and J. M. Harlan. 1986. An endothelial cell surface factor(s) induced in vitro by lipopolysaccharide, interleukin 1, and tumor necrosis factor-α increases neutrophil adherence by a CD18-dependent mechanism. *J. Immunol.* 136:4548–4553.

53. Moser, R., B. Schleiffenbaum, P. Groscurth, and J. Fehr. 1989. Interleukin-1 and tumor necrosis factor stimulate human vascular endothelial cells to promote transendothelial neutrophil passage. *J. Clin. Invest.* 83:444–445.

54. Entman, M. L., K. Youker, S. B. Shappell, C. Siegel, R. Rothiein, W. J. Dreyer, F. C. Schmalstieg, and C. W. Smith. 1990. Neutrophil adherence to isolated adult canine myocytes. *J. Clin. Invest.* 85:1497–1506.

55. Engler, R. L., G. W. Schmid-Schonbein, and R. S. Pavelec. 1983. Leukocyte capillary plugging in myocardial ischemia and reperfusion in the dog. *Am. J. Pathol.* 111:98–111.

56. Engler, R. L., M. D. Dahlgren, D. D. Morris, M. A. Peterson, and G. W. Schmid-Schonbein. 1986. Role of leukocytes in response to acute myocardial ischemia and reflow in dogs. *Am. J. Physiol.* 251:H314–H322.

57. Engler, R., and J. W. Covell. 1987. Granulocytes cause reperfusion ventricular dysfunction after 15-minutes of ischemia in the dog. *Circ. Res.* 61:20–28.

58. Reynolds, J. M., and P. F. McDonagh. 1989. Early in reperfusion, leukocytes alter perfused coronary capillarity and vascular resistance. *Am. J. Physiol.* 256. 25:H982–H989.

59. Romson, J. L., B. G. Hook, S. L. Kunkel, G. D. Abrams, M. A. Schork, and B. R. Lucchesi. 1983. Reduction of the extent of ischemic myocardial injury by neutrophil depletion in the dog. *Circulation.* 67:1016–1023.

60. Simpson, P. J., R. F. Todd III., J. C. Fantone, J. K. Mickelson, J. D. Griffin, and B. R. Lucchesi. 1988. Reduction of experimental canine myocardial reperfusion injury by a monoclonal antibody (anti-Mo1, anti-CD11b) that inhibits leukocyte adhesion. *J. Clin. Invest.* 81:624–629.

61. Bachwich, P. R., S. W. Chensue, J. W. Larrick, and S. L. Kunkel. 1986. Tumor necrosis factor stimulates interleukin 1 and prostaglandin E_2 production in resting macrophages. *Biochem. Biophys. Res. Commun.* 136:94–101.

62. Huber, M., B. Beutler, and D. Keppler. 1988. Tumor necrosis factor α stimulates leukotriene production in vivo. *Eur. J. Immunol.* 18:2085–2088.

63. Meyer, J. D., R. W. Yurt, R. Duhaney, D. G. Hesse, K. J. Tracey, Y. Fong, M. Verma, G. T. Shires, P. Dineen, S. F. Lowry, et al. 1988. Tumor necrosis factor-enhanced leukotriene B_4 generation and chemotaxis in human neutrophils. *Arch. Surg.* 123:1454–1458.

64. Sun, X. M., and W. Hsueh. 1988. Bowel necrosis induced by tumor necrosis factor in rats is mediated by platelet activating factor. *J. Clin. Invest.* 81:1328–1331.60.

65. Tsujimoto, M., S. Yokota, J. Vilcek, and G. Weissmann. 1986. Tumor necrosis factor provokes superoxide anion generation from neutrophils. *Biochem. Biophys. Res. Commun.* 137:1094–1100.

66. Ezra, D., L. M. Boyd, G. Feuerstein, and R. E. Goldstein. 1983. Coronary constriction by leukotriene C_4, D_4, and E_4 in the intact pig heart. *Am. J. Cardiol.* 51:1451–1454.

67. Mullane, K. M., and D. Fornabaio. 1988. Thromboxane synthetase inhibitors reduce infarct size by a platelet-dependent, aspirin-sensitive mechanism. *Circ. Res.* 62:668–678.

68. Mullane, K. M., M. A. Hatala, R. Kraemer, W. Sessa, and W. Westlin. 1987. Myocardial salvage induced by REV-5901, an inhibitor and antagonist of the leukotrienes. *J. Cardiovasc. Pharmacol.* 10:398–406.

69. Mullane, K. M., N. Read, J. A. Salmon, and S. Moncada. 1984. Role of leukocytes in acute myocardial infarction in anesthetized dogs: relationship to myocardial salvage by anti-inflammatory drugs. *J. Pharmacol. Exp. Ther.* 288:510–522.

70. Przyklenk, K., and R. A. Kloner. 1986. Superoxide dismutase plus catalase improve contractile function in the canine model of "stunned myocardium." *Circ. Res.* 58:148–156.

71. Chung, M. K., T. Gulick, R. E. Rotondo, G. F. Schreiner, and L. G. Lange. 1990. Mechanisms of cytokine inhibition of B-adrenergic agonist stimulation of cyclic AMP in rat cardiac myocytes: Impairment of signal transduction. *Circ. Res.* 67:753–763.

72. Rankin, J. S., P. A. Mchale, C. E. Arentzen, D. Ling, J. C. Greenfield, and R. W. Anderson. 1976. The three-dimensional dynamic geometry of the left ventricle in the conscious dog. *Circ. Res.* 39:304–313.